

Original Research

# The Effects of *Ginkgo biloba* Extract on Autophagy in Human Macrophages Stimulated by Cigarette Smoke Extract

Pengfei Zhang<sup>1,†</sup>, Junbao Zhu<sup>1,†</sup>, Linjie Zhang<sup>2</sup>, Xiaolan Lv<sup>3</sup>, Dongwei Guo<sup>1</sup>, Lijun Liao<sup>1</sup>, Shigao Huang<sup>4,\*</sup>, Zheng Peng<sup>5,\*</sup><sup>1</sup>Department of Pulmonary and Critical Care Medicine, Liuzhou Traditional Chinese Medical Hospital, 545001 Liuzhou, Guangxi, China<sup>2</sup>Institute for Stroke and Dementia, Ludwig-Maximilians-Universität München, 80539 Munich, Germany<sup>3</sup>Department of Clinical Laboratory, Liuzhou Maternity and Child Healthcare Hospital, 545001 Liuzhou, Guangxi, China<sup>4</sup>Department of Radiation Oncology, The First Affiliated Hospital, Air Force Medical University, 710032 Xi'an, Shaanxi, China<sup>5</sup>Department of Clinical Laboratory, Liuzhou Traditional Chinese Medical Hospital, 545001 Liuzhou, Guangxi, China\*Correspondence: [huangshigao2010@aliyun.com](mailto:huangshigao2010@aliyun.com) (Shigao Huang); [pengzheng@live.com](mailto:pengzheng@live.com) (Zheng Peng)

†These authors contributed equally.

Academic Editor: Jae Man Lee

Submitted: 26 September 2022 Revised: 5 January 2023 Accepted: 10 January 2023 Published: 15 March 2023

## Abstract

**Objective:** To investigate the effects of *Ginkgo biloba* extract (GBE) on autophagy in human macrophages stimulated by cigarette smoke extract (CSE). **Methods:** The human monocyte cell line U937 was cultured *in vitro*, and phorbol ester (PMA) was added to the cell culture medium to induce differentiation into human macrophages. CSE was prepared by traditional methods for experiments. The cells were divided into four groups: the blank group, the CSE model group, the GBE + CSE group, and the rapamycin + CSE group. Immunofluorescence was used to identify human macrophages, transmission electron microscopy was used to observe the ultrastructure of human macrophages in each group, ELISA was used to measure the amount of IL-6 and IL-10 in the supernatant from each group of cells, the mRNA levels of p62, ATG5, ATG7, and Rab7 were measured by real-time qPCR, and the protein expression levels of p62, ATG5, ATG7, and Rab7 were measured by Western blotting. **Results:** U937 cells were successfully differentiated into human macrophages after induction with PMA. The CSE model group had many more autophagosomes than the blank group. Compared with the CSE model group, the GBE + CSE group and the rapamycin + CSE group had significantly more autophagolysosomal. Compared with the other groups, the CSE model group had a higher level of IL-6 but a lower level of IL-10 in the supernatant ( $p < 0.05$ ). Compared with the blank group, the mRNA and protein expression levels of p62 in the CSE model group were significantly decreased, while the mRNA and protein expression levels of ATG5 and ATG7 were significantly increased in the CSE model group ( $p < 0.05$ ). No difference was found in the mRNA and protein expression levels of Rab7 between the blank group and the CSE model group. Compared with the CSE model group, the IL-6 level in the GBE + CSE group and the rapamycin + CSE group cell culture supernatant decreased significantly, p62 mRNA and protein expression significantly decreased, while ATG5, ATG7, and Rab7 mRNA and protein expression levels were significantly increased ( $p < 0.05$ ). Moreover, increased LC3-II/LC3-I ratio were also found in the GBE + CSE group and the rapamycin + CSE group compared with the CSE model group. **Conclusions:** GBE could promote the fusion of autophagosomes and lysosomes in human macrophages, enhance the autophagy function of human macrophages, and reduce the damaging effect of CSE on the autophagy function of macrophages.

**Keywords:** *Ginkgo biloba* extract; cigarette smoke extract; human macrophages; autophagy

## 1. Introduction

Chronic obstructive pulmonary disease (COPD) is a highly disabling chronic respiratory disease characterized by persistent respiratory symptoms and airflow limitation caused by airway and/or alveolar abnormalities. From 1980 to 2017, COPD was the third leading cause of death in the world, and the mortality rate will continue to increase in the next 20 years [1]. Chronic and long-period inhalation of cigarette smoke (CS) is considered a major cause of COPD [2]. CS can alter airway epithelial barrier function, increase oxidative stress, promote airway epithelial aging and activate proinflammatory pathways [3]. CS triggers the recruitment of blood monocytes to the lung, leading to an in-

crease in macrophages in the alveoli and lung parenchyma of COPD patients [4]. Macrophages play an important role in the innate and adaptive immune responses to alien particles and pathogens [5], and alveolar macrophages (AMs) are responsible for recognizing, phagocytosing and destroying pathogens and processing inhaled particulate matter (including cigarette smoke). The key innate immune effector cells, AMs, play a key role in initiating and maintaining chronic inflammatory responses, and at the same time they play an important role in the pathogenesis of chronic inflammation and abnormal repair in COPD [6]. It was found that the AMs of smokers and COPD patients have functional defects, and CS can impair the phagocytic function



of AMs by influencing their autophagy function, reducing their ability to clear airway bacteria [7].

Autophagy, an automatic cellular component degradation system performed by lysosomes, promotes the recycling of damaged intracellular organelles, denatured proteins and other biological macromolecules, and is essential for maintaining the intracellular environment and cell survival [8]. In addition to regulating inflammatory responses by maintaining protein and organelle homeostasis and cell viability [9], autophagy also plays a key role in regulating the proliferation, recruitment, polarization and phagocytosis of macrophages [10]. CS exposure leads to protein deposition dysfunction resulting in the accumulation of ubiquitinated proteins and impairs the function of a key player in autophagy, p62. CS-induced autophagy impairment accelerates lung aging and COPD emphysema exacerbation, which is a potential mechanism to initiate the pathogenesis of COPD emphysema [11]. Studies have found that CSE can inhibit the maturation and degradation of autophagosomes in macrophages, inhibit autophagic flux, lead to defective autophagosome maturation and abnormal accumulation of autophagosomes in macrophages, and damage the normal autophagy function of macrophages [12]. GBE is a mixture containing a variety of effective medicinal ingredients extracted from the dried leaves of *Ginkgo biloba*. Previous studies have found that GBE can reduce the levels of inflammatory factors in the bronchoalveolar lavage fluid (BALF) and serum of COPD rats [13], but the specific mechanism is still unclear. In this study, CSE-stimulated human macrophages were used to establish a COPD cell model *in vitro* to investigate whether GBE could enhance the autophagy function of human macrophages and to explore the possible mechanism of GBE in the treatment of COPD.

## 2. Materials and Methods

### 2.1 Cells and Main Reagents

Human histiocytic lymphoma cells (U937 cells) were purchased from Shanghai Zhongqiao Xinzhou Biotechnology Co., Ltd. (Item No.: ZQ0087, Shanghai, China); phorbol ester (PMA) was produced by Dalian Meilun Biotechnology Co., Ltd. (Item No.: MB5349, Dalian, China). *Ginkgo biloba* extract was purchased from Hebei Shenwei Pharmaceutical Group Co., Ltd. (Z13020795, Shijiazhuang, China). Rapamycin was purchased from Dalian Meilun Biotechnology Co., Ltd. (lot No.: MB1197, Dalian, China), and filter cigarettes were produced by Hongyun Honghe Tobacco Co., Ltd. (tar content 10 mg, smoke nicotine content 1.1 mg, smoke carbon monoxide content 12 mg, Kunming, China). IL-6 (lot No.: H201127-007a) and IL-10 (lot No.: H201127-009a) ELISA kits were purchased from Shenzhen Xinbosheng Biotechnology Co., Ltd. (Shenzhen, China), and SYBR FAST qPCR Master Mix (product number: KM4101) was purchased from KAPA Company (Woburn, MA, USA) in the United States.

Primary antibodies against p62 (lot No.: bs-55207R), ATG5 (lot No.: bs-4005R), ATG7 (lot No.: bs-2432R), Rab7 (lot No.: bs-6703R), and CD68 (lot No.: bs-0649R) were purchased from Beijing Boaosen Biotechnology Co., Ltd (Beijing, China).

### 2.2 Methods

#### 2.2.1 Preparation of 100% CSE

Referring to the method of Li Minjing *et al.* [14], first, a piece of unfiltered cigarette (tar content 10 mg, smoke nicotine content 1.1 mg, smoke carbon monoxide content 12 mg) was ignited. One end of a rubber tube was connected to a cigarette filter, and the other end of the rubber tube was connected to a 50 mL syringe. The syringe was pulled slowly 2–3 times first, and when the smoke in the tube was thick, the syringe was slowly pulled and cigarette smoke was collected in the syringe (each syringe collects 50 mL, 1 cigarette produces 8 tubes, or approximately 400 mL), and was injected into 20 mL RPMI1640 medium containing 10% fetal bovine serum. The samples were allowed to sit until the cigarette smoke was fully dissolved by sufficient shaking, and the above method was repeated 4 times. The pH value was adjusted to 7.4 with 1 mol/L NaOH solution and sterilized by filtration through a 0.22  $\mu\text{m}$  filter membrane, and the obtained suspension was defined as 100% CSE stock solution. In this experiment, human macrophages were treated with CSE at a concentration of 15%.

#### 2.2.2 Culture and Induction of Differentiation of U937 Cells

U937 cells were cultured in RPMI 1640 medium containing 10% fetal bovine serum (FBS) at a temperature of 37 °C and a CO<sub>2</sub> concentration of 5% and passaged once every 2 days; the U937 cells were first resuspended and counted. The cells were evenly seeded into 6-well plates, the number of cells seeded in each well was approximately  $1 \times 10^6$ , and PMA (50 ng/mL) was added for induction for 24 h.

#### 2.2.3 Identification of Human Macrophages

CD68 is a lysosome-associated membrane protein and the most well-known panmacrophage marker, often used as a specific marker for identifying macrophages [15]. After the U937 cells were induced to differentiate with PMA for 24 h, the expression of CD68 was measured by immunofluorescence staining to identify whether U937 cells differentiated into human macrophages; the original medium was aspirated, digested with trypsin, resuspended and counted, and the cells were seeded in a 24-well plate. The plate contained approximately  $1 \times 10^6$  cells per well. After the cells adhered to the wall for a period of time and the confluency was approximately 80% to 90% under a light microscope, they were rinsed with phosphate buffer saline (PBS), fixed with 4% paraformaldehyde at room temperature, permeabilized with 0.5% Triton X-100 at room temperature for 20

**Table 1. Primer sequences of *p62*, *ATG5*, *ATG7*, *Rab7*, and *GAPDH* used in this study.**

Gene name	Direction	Primer sequence (5' to 3')	Product length (bp)
<i>p62</i>	Forward	AAGAGAAAAAAGAGTGCCG	232
	Reverse	TCAGACAGGTGCCCGA	
<i>ATG5</i>	Forward	GCAACTCTGGATGGGATT	170
	Reverse	CAGCCACAGGACGAAAC	
<i>Rab7</i>	Forward	CAAAGCCACAATAGGAGC	152
	Reverse	ATACCAGAACGCAGCAGT	
<i>ATG7</i>	Forward	AGTTGTTTGCTCCGTGAC	141
	Reverse	CCTCCTTTCTGGTCTTTT	
<i>GAPDH</i>	Forward	GGGAAACTGTGGCGTGAT	299
	Reverse	GAGTGGGTGTCGCTGTTGA	

min, and blocked with 5% Bovine Serum Albumin (BSA) at 37 °C for 1 h. Diluted CD68 primary antibody was added to the cells and incubated at 4 °C overnight. The cells were incubated with secondary antibody at 37 °C for 1 h, washed with PBS, and mounted with anti-fluorescence quenching mounting solution (DAPI). The expression of CD68 antibody was observed under a fluorescence microscope (inverted laboratory microscope, Leica DM IL LED, Leica, Germany); the judging criterion was that the cytoplasm of successfully differentiated cells was stained red, and the cytoplasm of undifferentiated cells was not stained.

#### 2.2.4 Grouping and Drug Intervention

The well-grown human macrophages were randomly divided into 4 groups: the blank group: cultured with culture medium for 48 h; the CSE model group: after culturing with culture medium for 24 h, CSE at a final concentration of 15% was added for another 24 h; the GBE + CSE group: after culturing for 24 h with GBE at a final concentration of 1.75 µg/mL and then adding CSE at a final concentration of 15% for another 24 h; the Rapamycin + CSE group: after culturing for 24 h with rapamycin at a final concentration of 200 ng/mL, CSE at a final concentration of 15% was added for another 24 h. In the experiment, CSE, GBE and rapamycin were all diluted with RPMI 1640 medium containing 10% FBS, and the volume of the culture medium in each group was the same.

#### 2.2.5 Observation of the Ultrastructure of Human Macrophages in Each Group by Transmission Electron Microscopy

After drug intervention, the culture medium was removed by suction, and the cells were washed with PBS and digested with trypsin. After centrifugation, the cells were allowed to sink to the bottom of the centrifuge tube. The supernatant was removed by suction, fixed with 2.5% glutaraldehyde, placed at 4 °C, and then treated with 1% osmic acid. The samples were fixed, dehydrated with ethanol and acetone, impregnated with acetone and pure epoxy resin, embedded, polymerized, ultrathin sectioned, and then stained with uranyl acetate and lead citrate in the dark. The

macrophage ultrastructure was observed and photographed under a transmission electron microscope (TEM) (Hitachi HT7700, Tokyo, Japan).

#### 2.2.6 ELISA to Measure the Content of IL-6 and IL-10 in the Supernatant from Each Group of Cells

After drug intervention, the cell culture supernatants from each group were collected, and ELISA was used to measure the contents of IL-6 and IL-10 in the cell supernatants from each group. The specific operations were carried out according to the kit instructions.

#### 2.2.7 The mRNA Levels of *p62*, *ATG5*, *ATG7*, and *Rab7* in Human Macrophages in Each Group were Measured by q-PCR

The cells were collected from each group, the total RNA was extracted according to the instructions of the TRIzol reagent, the RNA was reverse-transcribed into cDNA and the product was stored at 4 °C for later use. The cDNA was used as the template for PCR amplification, and PCR was carried out according to the following conditions: Pre-denaturation at 95 °C for 3 min, denaturation at 95 °C for 5 s, annealing at 56 °C for 10 s, extension at 72 °C for 25 s, and amplification for 40 cycles. The relative expression levels of *p62*, *ATG5*, *ATG7*, and *Rab7* mRNA were calculated by the  $2^{-\Delta\Delta Ct}$  method with *GAPDH* as the internal reference. The experiment was repeated three times. Please refer to Table 1 for primer sequence information.

#### 2.2.8 Western Blot (WB) Analysis of *p62*, *ATG5*, *ATG7*, *Rab7*, and LC3 Protein Expression in Human Macrophages in Each Group

The cells from each group were collected, and 200 µL of lysis buffer containing protease and phosphatase inhibitors was added to  $1 \times 10^6$  cells to fully lyse and extract the total protein. The protein concentration was determined by the BCA method. After separation by PAGE electrophoresis, the membrane was transferred by the wet transfer method at 90 V for 50 min and blocked with 5% nonfat milk powder at room temperature for 2 h. Then, primary antibody (1:1000) was added and incubated at 4

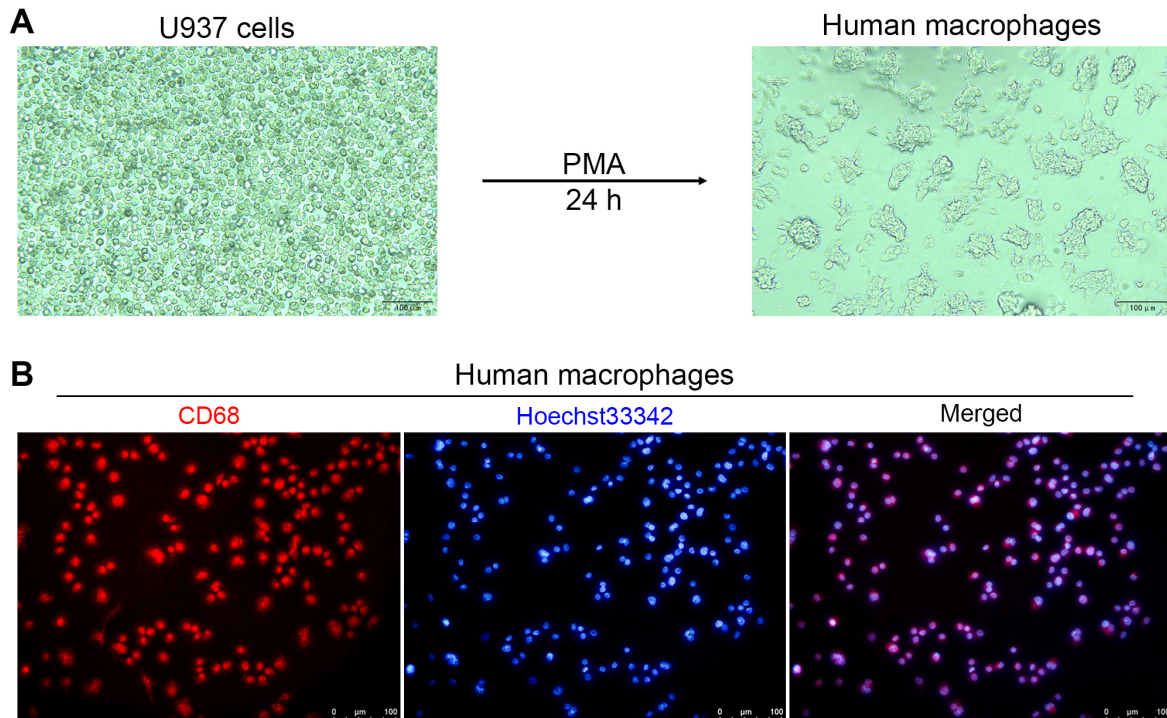


**Fig. 1. Almost all U937 cells were differentiated into macrophages after 24 h of induction with PMA.** (A) Representative live-cell images demonstrating the morphological differences between U937 cells (left) and macrophages (right). (B) Representative IF staining images of CD68 in human macrophages. Nuclei were visualized using Hoechst-33342 staining. Scale bars, 100 μm.

°C overnight, and the membrane was washed 3 times with PBS with Tween 20 (PBST) for 5 min each time. Goat anti-rabbit IgG antibody diluted at a ratio of 1:10,000 was added, incubated for 1 h at room temperature, and washed three times with PBST. The membrane was exposed in an automatic chemiluminescence analyzer in the dark room after incubation with the chemiluminescent substrate enhanced chemiluminescence (ECL). ImageJ software (National Institute of Health, Bethesda, MD, USA) was used to measure the absorbance and calculate the relative expression of the protein. The expression level was calculated relative to the internal reference protein.

### 3. Results

#### 3.1 Identification of Human Macrophages

In terms of cell morphology, U937 cells were round or oval under a light microscope and were small. They were suspended cells without protrusions or pseudopodia on the surface. After 24 h of differentiation induced by PMA, the cell morphology changed. The cell shapes were different, the volume was obviously increased, the cell aggregation phenomenon was obvious, and some cells grew pseudopodia. After immunofluorescence (IF) staining for CD68, the cell cytoplasm was obviously stained red, the nucleus was blue, and the cell differentiation rate reached more than 95%, which indicates that the U937 cells had differentiated and become human macrophages. Please refer to Fig. 1.

#### 3.2 GBE Increased Autophagolysosomes in CSE-Treated Macrophages as Shown by Transmission Electron Microscopy

Electron microscopy is still an important tool for observing autophagic activity and the ultrastructure of macrophages [16]. When certain organelles or local cytoplasm degenerate and disintegrate in cells they are surrounded by double-membrane, vesicle-like bodies called autophagosomes. After fusion with primary lysosomes, autophagolysosomes are formed, and hydrolases are activated to decompose aging organelles, proteins, mitochondria, glycogen and other substances, providing energy for cellular metabolism, maintaining cellular homeostasis and avoiding protein abnormalities. From the electron microscope results, it could be seen that there was autophagy in the blank group, with a small amount of autophagolysosomes, but no vacuolization, and the cell state was good [17–19]; the CSE model group had enhanced autophagy, with an obvious increase in autophagosomes, with relatively few autophagolysosomes, obvious vacuolization, and poor cell state [17–19]; the GBE + CSE group and the rapamycin + CSE group had significantly enhanced autophagy. Compared with the CSE model group, the number of autophagolysosomes was significantly increased in these two groups, with a few vacuoles in the cells, and the cell state was acceptable [17–19]. Please refer to Fig. 2, Table 2, and Fig. 3 for details.

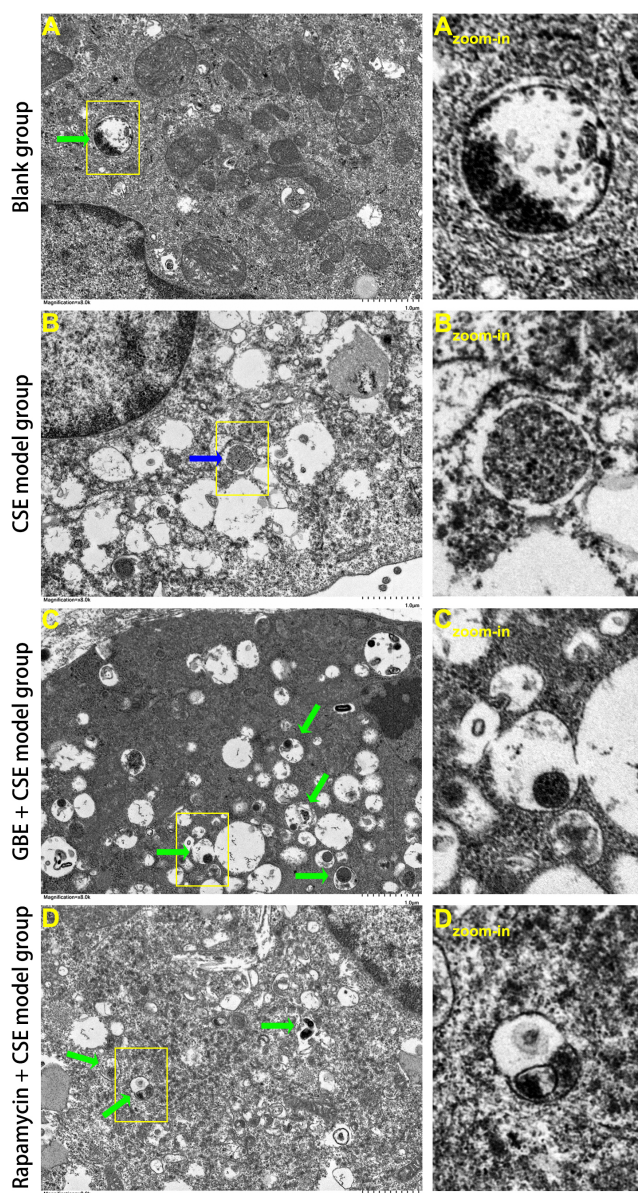


**Fig. 2. Representative images of the ultrastructure inside macrophages of different groups.** (A) Representative images of the ultrastructure of macrophages in the blank group. ( $A_{\text{zoom-in}}$ ) The zoom-in image of the structure indicated by the arrow. (B) Representative images of the ultrastructure of macrophages in the CSE model group. ( $B_{\text{zoom-in}}$ ) The zoom-in image of the structure indicated by the arrow. (C) Representative images of the ultrastructure of macrophages in the GBE + CSE group. ( $C_{\text{zoom-in}}$ ) The zoom-in image of the ultrastructure indicated by the corresponding arrows. (D) Representative images of the ultrastructure of macrophages in the rapamycin + CSE group. ( $D_{\text{zoom-in}}$ ) The zoom-in image of the ultrastructure indicated by the corresponding arrows. Green arrows: autophagolysosomes; blue arrows: autophagosomes. These photos were taken under a transmission electron microscope. Scale bars, 1  $\mu\text{m}$ .

### 3.3 ELISA to Measure the Content of IL-6 and IL-10 in the Supernatant from Each Group

Compared with the blank group, the content of IL-6 in the supernatant from the cells in the CSE model group was significantly increased, while the content of IL-10 in the cell supernatant was significantly decreased ( $p < 0.05$ ). Compared with the CSE model group, the content of IL-6 in the supernatant from the GBE + CSE group and the rapamycin + CSE group decreased significantly ( $p < 0.05$ ), but there was no significant difference in the content of IL-10 ( $p > 0.05$ ). Please refer to Table 3 and Fig. 4 for details.

### 3.4 RT-PCR Measurement of *p62*, *ATG5*, *ATG7*, and *Rab7* mRNA Levels in Human Macrophages in Each Group

Compared with the blank group, the CSE model group had higher expression levels of *ATG5* and *ATG7* mRNA and a lower level of *p62* mRNA in human macrophages ( $p < 0.05$ ); however, no difference was found in *Rab7* mRNA expression between them ( $p > 0.05$ ). Compared with the CSE model group, the expression levels of *ATG5*, *ATG7* and *Rab7* mRNA in human macrophages in the GBE + CSE group and rapamycin + CSE group were significantly increased, while the expression level of *p62* mRNA was significantly decreased ( $p < 0.05$ ). More importantly, GBE was more advantageous than rapamycin in reducing *p62* mRNA levels. Please refer to Table 4 and Fig. 5 for details.

### 3.5 Comparison of *p62*, *ATG5*, *ATG7*, *Rab7*, and *LC3* Protein Expression in Human Macrophages in Each Group

Compared with the blank group, the protein expression levels of *ATG5* and *ATG7* in human macrophages in the CSE model group were significantly increased, while the protein expression of *p62* was significantly decreased ( $p < 0.05$ ). No difference was found between them in the expression of *Rab7* ( $p > 0.05$ ). Compared with the CSE model group, the expression levels of *ATG5*, *ATG7* and *Rab7* proteins in human macrophages in the GBE + CSE group and the rapamycin + CSE group were significantly increased, while the protein expression levels of *p62* were significantly decreased ( $p < 0.05$ ). Compared with the blank group, the ratio of LC3II/LCI in all the other three groups showed an increase, among which the ratios of GBE and rapamycin group displayed a higher increase than the CSE model group ( $p < 0.001$ ). Please refer to Table 5 and Fig. 6 for details.

## 4. Discussion

COPD is a disease characterized by progressive airflow obstruction primarily caused by chronic inhalation of CS, and CS exposure induces oxidative stress, resulting in transcription factor activation and increased expression of inflammatory mediators and proteases [20]. In addition, smoking can be a major cause of COPD by impairing the mucus transport system of the airway, impairing cough reflex sensitivity, and inducing inflammation [21].

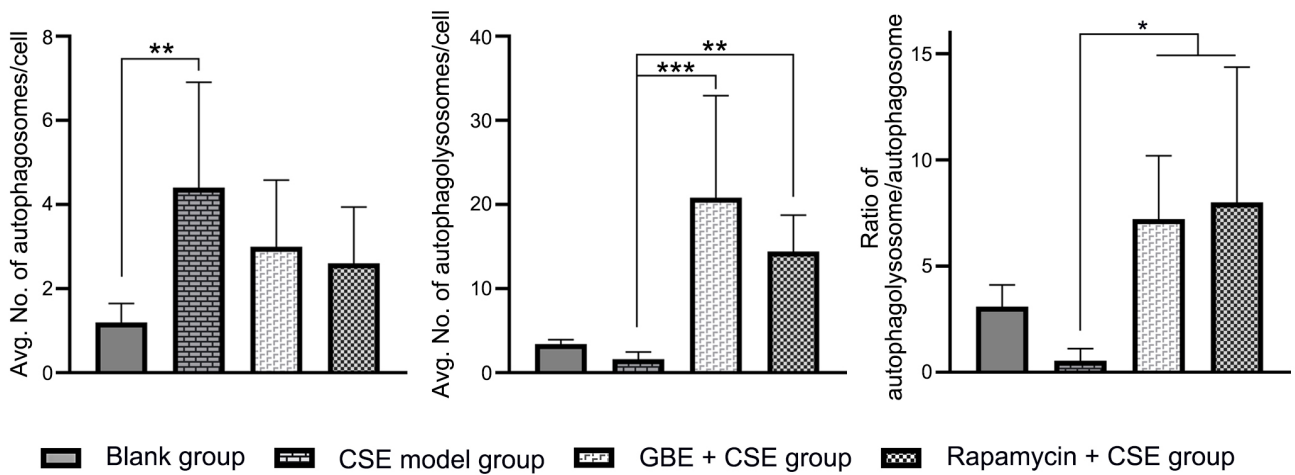


**Fig. 3. GBE or rapamycin increased autophagolysosomes in CSE-treated macrophages.** Bar graphs showing the average number of autophagosome, autophagolysosome, and the ratio of autophagolysosomes VS. autophagosomes in macrophages of different groups. One-way Analysis of Variance (ANOVA) and Tukey's multiple comparisons test were performed. \*  $p < 0.05$ , \*\*  $p < 0.01$ , \*\*\*  $p < 0.001$ .

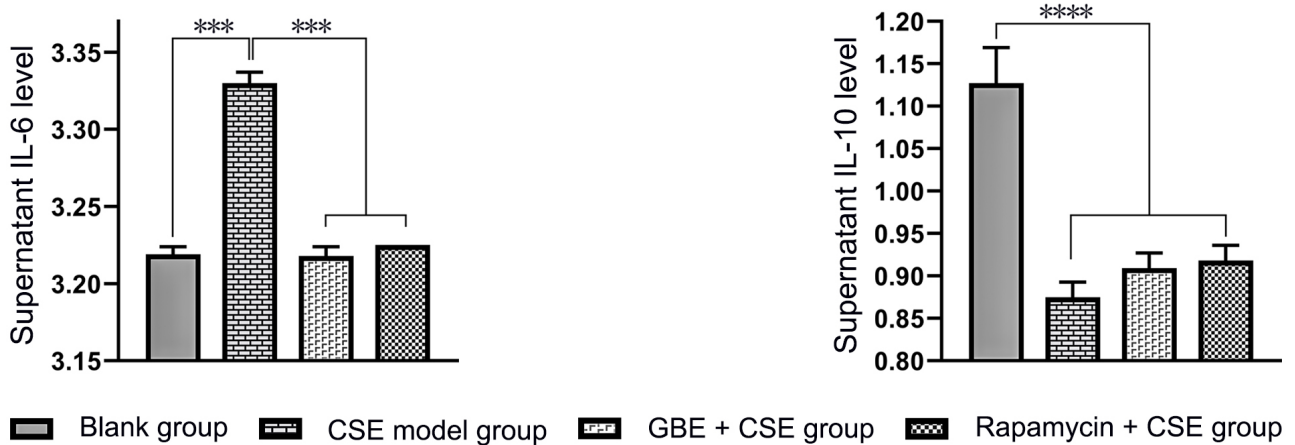


**Fig. 4. Bar graphs showing the differences between IL-6 and IL-10 in the supernatants from each group.** One-way ANOVA and Tukey's multiple comparisons test were performed. \*\*\*  $p < 0.001$ , \*\*\*\*  $p < 0.0001$ .

**Table 2. The average number of autophagosome, autophagolysosome, and the ratio of autophagolysosomes VS. autophagosomes in macrophages of different groups.**

Groups	Autophagosome	Autophagolysosome	Autophagolysosome/Autophagosome
Blank group	1.200 ± 0.447	3.400 ± 0.548	3.100 ± 1.025
CSE model group	4.400 ± 2.510	1.600 ± 0.894	0.558 ± 0.568
GBE + CSE group	3.000 ± 1.581	20.800 ± 12.153	7.213 ± 2.992
Rapamycin + CSE group	2.600 ± 1.342	14.400 ± 4.336	8.000 ± 6.386

**Table 3. IL-6 and IL-10 levels in the cell supernatants from each group.**

Group	IL-6	IL-10
Blank group	3.219 ± 0.005	1.127 ± 0.042
CSE model group	3.330 ± 0.007	0.875 ± 0.018
GBE + CSE group	3.218 ± 0.006	0.909 ± 0.018
Rapamycin + CSE group	3.225 ± 0.000	0.918 ± 0.018

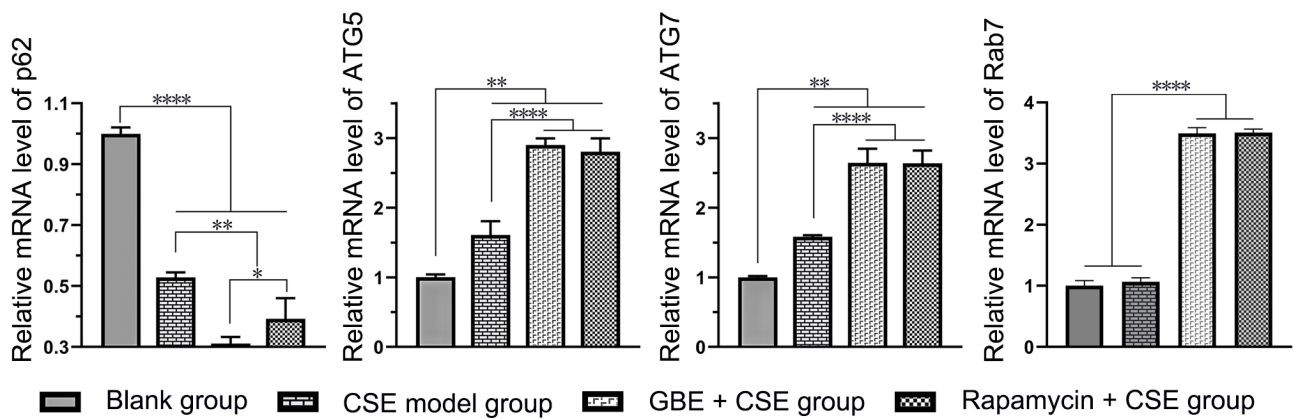


**Fig. 5.** Bar graphs showing the differences in the mRNA expression levels of *p62*, *ATG5*, *ATG7*, and *Rab7* in human macrophages among each group. One-way ANOVA and Tukey's multiple comparisons test were performed. \*  $p < 0.05$ , \*\*  $p < 0.01$ , \*\*\*\*  $p < 0.0001$ .

**Table 4.** The mRNA expression levels of *p62*, *ATG5*, *ATG7*, and *Rab7* in human macrophages in each group.

Group	<i>p62</i>	<i>ATG5</i>	<i>ATG7</i>	<i>Rab7</i>
Blank group	1.000 ± 0.021	1.001 ± 0.042	1.000 ± 0.018	1.002 ± 0.082
CSE model group	0.528 ± 0.017	1.608 ± 0.200	1.583 ± 0.024	1.065 ± 0.067
GBE + CSE group	0.311 ± 0.022	2.902 ± 0.094	2.644 ± 0.204	3.496 ± 0.093
Rapamycin + CSE group	0.392 ± 0.068	2.805 ± 0.191	2.637 ± 0.186	3.509 ± 0.057

**Table 5.** The protein levels of *p62*, *ATG5*, *ATG7*, *Rab7*, and *LC3* in human macrophages in each group.

Group	<i>p62</i>	<i>ATG5</i>	<i>ATG7</i>	<i>Rab7</i>	<i>LC3-II/LC3-I</i>
Blank group	0.579 ± 0.020	0.150 ± 0.006	0.159 ± 0.012	0.355 ± 0.025	0.290 ± 0.020
CSE model group	0.406 ± 0.034	0.298 ± 0.131	0.350 ± 0.054	0.367 ± 0.021	0.415 ± 0.016
GBE + CSE group	0.166 ± 0.011	0.846 ± 0.055	0.450 ± 0.034	0.483 ± 0.025	0.537 ± 0.019
Rapamycin + CSE group	0.160 ± 0.015	0.853 ± 0.021	0.469 ± 0.038	0.488 ± 0.037	0.530 ± 0.002

Therefore, in this study, CSE was used to stimulate human macrophages to construct an *in vitro* COPD cell model. Macrophages are a major group of innate immune cells present in various tissues, where they play an important role as sentinels of the immune system [22]. AMs are the main phagocytic and immunoregulatory innate immune cells in the airway, and their main function is to phagocytose and destroy invading pathogens, while the phagocytic function of macrophages in COPD patients is defective and cannot effectively remove pathogenic bacteria, which in turn leads to persistent bacterial colonization of the lower respiratory tract [23]. *In vitro* studies have shown that CSE can stimulate mouse AMs to secrete the chemokine ligands CXCL-1, CXCL-2 and IL-6 [24]. IL-6 is a multifunctional proinflammatory cytokine that plays a key role in the development of inflammatory responses [25]. IL-10 is an anti-inflammatory factor that inhibits the expansion of inflammatory responses [26]. In this study, the expression of the proinflammatory factor IL-6 in the cell supernatant from the CSE model group was significantly higher than that from the blank group, while the expression of the anti-inflammatory factor IL-10 was significantly decreased. Af-

ter the intervention of GBE and rapamycin, compared with the CSE model group, the content of IL-6 in the supernatant was significantly lower while the content of IL-10 was increased, indicating that CSE can stimulate macrophages to secrete inflammatory factors, while GBE and rapamycin can reduce the inflammatory stimulation effect of CSE on macrophages.

Autophagy is an automated cellular component degradation system performed by lysosomes that controls protein and organelle degradation for homeostasis [27]. There are three main types of autophagy: macroautophagy (often referred to as autophagy), microautophagy, and chaperone-mediated autophagy. Macroautophagy is the primary mechanism of autophagy that involves the utilization of transient double membrane vesicles called autophagosomes to recycle damaged proteins and organelles, and then these vesicles fuse with lysosomes, causing lysosomal acid hydrolases to degrade their contents [28]. Autophagy is critical in the regulation of innate and adaptive immune responses; it plays a key role in lung inflammation and the pathogenesis of many chronic lung diseases, and autophagy plays a central role in host defense through multiple mech-

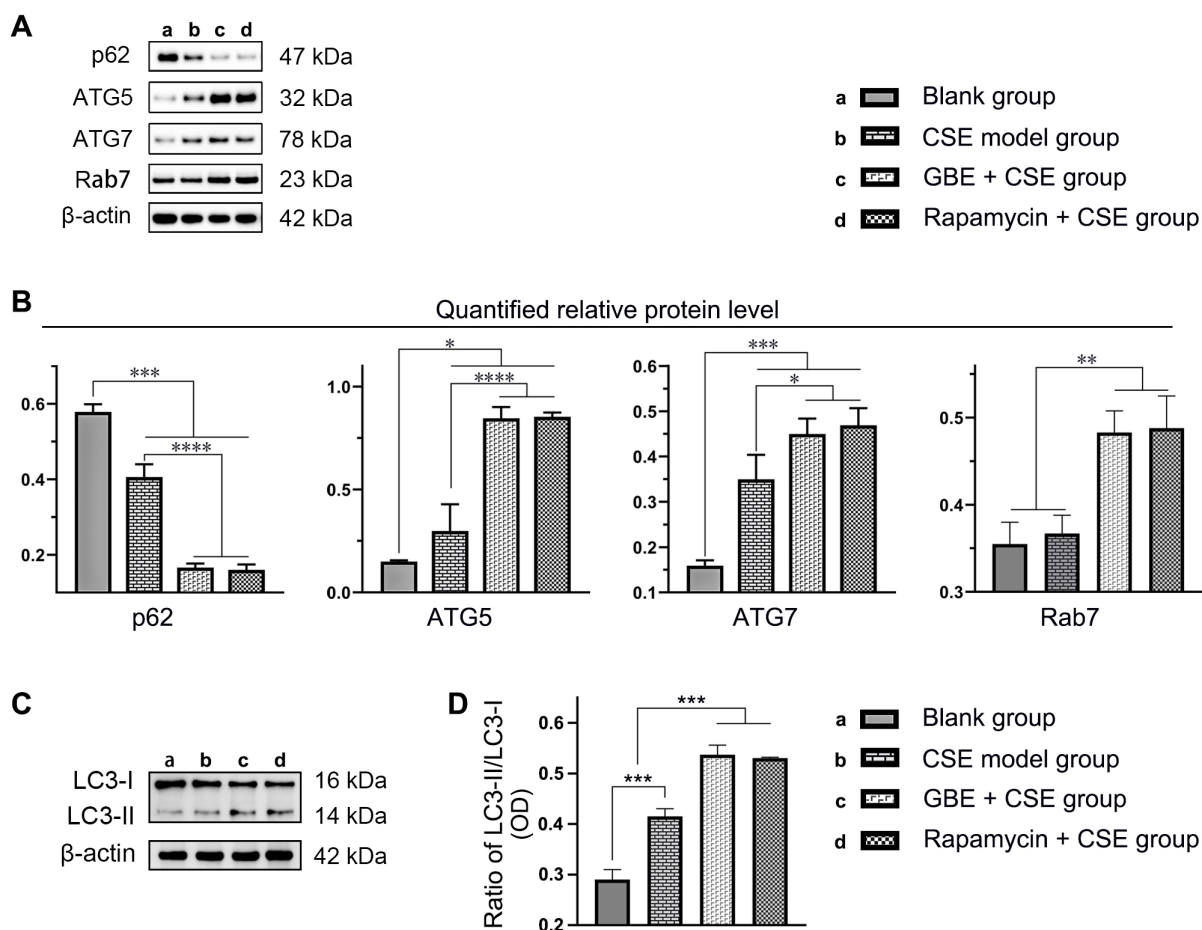


**Fig. 6. The protein level changes in p62, ATG5, ATG7, Rab7, and LC3 in human macrophages among each group.** (A) Representative WB results showing the protein levels of p62, ATG5, ATG7, and Rab7 in human macrophages of each group. (a) blank group; (b) CSE model group; (c) GBE + CSE group; (d) Rapamycin + CSE group. (B) Bar graphs showing the quantified protein expression levels results of p62, ATG5, ATG7, and Rab7 in human macrophages of each group. One-way ANOVA and Tukey's multiple comparisons test were performed. (C) Representative WB results showing the protein levels of LC3-I and LC3-II in human macrophages of each group. (a) blank group; (b) CSE model group; (c) GBE + CSE group; (d) Rapamycin + CSE group. (D) Bar graphs showing the ratio of LC3-II VS. LC3-I [optical density (OD) value] in human macrophages of each group. One-way ANOVA and Tukey's multiple comparisons test were performed. \*  $p < 0.05$ , \*\*  $p < 0.01$ , \*\*\*  $p < 0.001$ , \*\*\*\*  $p < 0.0001$ .

anisms [29]. Chronic exposure to CS-induced oxidative stress and inflammation leads to impaired autophagy, which in turn accelerates the pathogenesis of COPD emphysema [11]. Macrophages play a key role in the immune response and tissue repair in COPD [30]. AMs constitute the first line of the host innate immune response and play a critical role in early CS exposure. Autophagy mediates CS-initiated activation of macrophage matrix metalloproteinase 12 (MMP12) and subsequent airway epithelium injury, which is an important mechanism to induce the occurrence and development of airway inflammation in COPD [31]. CSE can induce autophagic injury in lung macrophages and cause lung macrophage dysfunction, which on the one hand leads to a decline in their phagocytic function and bacterial clearance capacity and on the other hand promotes the release of inflammatory mediators and proteases [32].

P62 is a multifunctional adaptor protein that is generally considered to play a key role in autophagy [33]. As one of the markers of autophagy, it is often used to determine the state of autophagy. When autophagy is activated, the level of p62 protein is low, while the p62 level is high when autophagy is inhibited [34]. ATG proteins play a key role in regulating the process and activity of autophagy [35] and constitute the most important molecular platform that plays a central role in autophagy by regulating the initiation and maturation of autophagosomes [36]. ATG5 and ATG7 are key ATG proteins [37], and the expression of ATG5 and ATG7 proteins increases significantly when autophagy is activated [38]. ATG5 maintains normal developmental processes by mediating various signals and is a core component of autophagy [39]. It has been reported that ATG5 plays a key role in autophagosome formation

and that free ATG5 can facilitate the formation of more autophagosomes [40]. Fluctuations in ATG5 levels largely affect autophagy and are directly involved in the formation of autophagosomes [41]. ATG7 is essential for autophagy, drives the binding of ATG12 to ATG5, and binds LC3-I to lipids of phosphatidylethanolamine to generate LC3-II [42]. Rab7 (or Ypt7 in yeast) is one of the conserved housekeeping Rabs in all eukaryotes and acts as a master regulator of membrane trafficking in eukaryotes. Localized in late endosomes and lysosomes, Rab7 plays a key role in the autophagosome-lysosome fusion step [43,44]. Its deletion of lysosomes could cause a reduction in the number of lysosomes fused to autophagosomes, which in turn could lead to autophagolysosome maturation impairment [45].

In this study, compared with the blank group, the mRNA and protein expression levels of ATG5 and ATG7 in human macrophages of the CSE model group were significantly increased, and the mRNA and protein expression levels of p62 were significantly decreased, indicating that autophagy was induced after CSE treatment, with increased autophagosomes. Compared with the CSE model group, the mRNA and protein expression levels of ATG5, ATG7, and Rab7 in human macrophages in the GBE + CSE group and the rapamycin + CSE group were significantly increased, while the mRNA and protein expression levels of p62 were significantly decreased, indicating that autophagy was further enhanced by the addition of GBE or the autophagy agonist rapamycin. However, no difference in the expression of Rab7 mRNA or protein levels was found between the blank group and the CSE model group. Moreover, the levels of Rab7 in the CSE model group were significantly lower than those in the GBE + CSE group and the rapamycin + CSE group, indicating that the number of autophagolysosomes was relatively deficient and that there were impaired autophagosome maturation in the CSE model group. In the CSE model group, ATG5, a key protein in autophagosome formation, was significantly increased compared with the blank group, while Rab7, one of the main indicators of lysosome quantity, had no significant difference compared with the blank group. These results indicated that CSE intervention can cause relatively insufficient lysosome formation, a reduced number of autophagolysosomes, and impaired autophagosome maturation in macrophages, which in turn affects normal metabolism in macrophages.

Autophagy is dependent on the lysosomal degradation pathway and plays a crucial role in the development of COPD [46]. Defective autophagy fails to completely clear aged or defective mitochondria, misfolded or damaged protein aggregates, and autophagosomes through lysosomes, thereby further disrupting the cellular clearance process, which drives the initiation and progression of COPD [47]. CS can trigger active autophagy but cause insufficient autophagic clearance in the lung, resulting in a significant accumulation of autophagosomes [48]. Monick found that

CS impairs autophagy in AMs in COPD patients, and this autophagy impairment leads to reduced protein aggregation clearance, mitochondrial dysfunction, and defective bacterial delivery to lysosomes [49]. Another study found that CS exposure enhanced the autophagy process, which could cause insufficient autophagic clearance in macrophages, resulting in an increase in autophagic proteins [50].

In this study, the level of autophagy in the CSE model group was significantly changed compared with the blank group, as suggested by the increased expression of autophagy related proteins. Moreover, under the electron microscope, the number of autophagosomes in macrophages in the CSE model group was significantly increased compared with that in the blank group, but the formation of autophagolysosomes was less, indicating that there is a fusion barrier between autophagosomes and lysosomes in the CSE model group, resulting in defective autophagy, which in turn causes abnormal aggregation of proteins and autophagosomes, hinders the transmission of damaged organelles to lysosomes, further affects the normal metabolism of macrophages, and eventually leads to a poor cell state and obvious vacuolation. Compared with that in the CSE model group, autophagy was further activated in the GBE + CSE group and the rapamycin + CSE group, and the expression of the autophagy proteins ATG5, ATG7, and Rab7 was significantly increased. Under an electron microscope, the number of autophagolysosomes in human macrophages in the GBE + CSE group and rapamycin + CSE group was significantly higher than that in the CSE model group. Hence, we can conclude that GBE and rapamycin can promote the fusion of autophagosomes and lysosome bodies, accelerate the removal of aging mitochondria, damaged protein aggregates and autophagosomes, and thereby maintain the autophagy function of macrophages.

Nonetheless, there are some limitations in this study. First, due to limited resources, the design of this study is relatively simple. Second, the methods used in this study to reflect autophagic activity have their own limitations. For example, although ATG protein levels are increased in other groups with different treatments compared with the blank group, this alone is not sufficient to conclude that autophagy is being induced, but rather suggestive of the changes in autophagy caused by these treatments. Besides, in addition to TEM, other techniques would be necessary to be performed to further confirm the hypothesis, such as quantifying the percentage of autophagolysosomes using LysoTracker reagent or indirect immunofluorescence against Lamp1. Third, the CSE exposure time used to establish the COPD model is relatively short compared with the real situation in patients which usually takes years.

## 5. Conclusions

In conclusion, we find that GBE can promote the fusion of autophagosomes and lysosomes in macrophages, enhance the autophagy function of macrophages, and re-

duce the damage to the autophagy function by CSE in macrophages. This study provides a new perspective for the treatment of COPD.

### Availability of Data and Materials

All data needed to evaluate the conclusions are present in the paper.

### Author Contributions

ZP, SH, and PZ conceptualized the idea. PZ, JZ, and ZP designed the research studies. PZ and JZ conducted the experiments, and LZ, XL, DG, and LL helped with the experiments. PZ provided resource, and DG helped resource. PZ and ZP analyzed the data. PZ, SH, and ZP wrote the manuscript. All authors contributed to editorial changes in the manuscript. All authors read and approved the final manuscript.

### Ethics Approval and Consent to Participate

Not applicable.

### Acknowledgment

We sincerely thank Professor Yuping Tan (Guangxi University of Chinese Medicine, Nanning, China) for her great help in the establishment of research model and guidance in the previous study.

### Funding

This work is funded by National Natural Science Foundation of China (No. 81904111), and Guangxi Natural Science Foundation (No. 2020GXNSFBA297022).

### Conflict of Interest

The authors declare no conflict of interest.

### References

- [1] GBD 2017 Causes of Death Collaborators. Global, regional, and national age-sex-specific mortality for 282 causes of death in 195 countries and territories, 1980-2017: a systematic analysis for the Global Burden of Disease Study 2017. *Lancet*. 2018; 392: 1736–1788.
- [2] Nucera F, Mumby S, Paudel KR, Dharwal V, DI Stefano A, Casolaro V, *et al*. Role of oxidative stress in the pathogenesis of COPD. *Minerva Medica*. 2022; 113: 370–404.
- [3] Liu A, Zhang X, Li R, Zheng M, Yang S, Dai L, *et al*. Overexpression of the SARS-CoV-2 receptor ACE2 is induced by cigarette smoke in bronchial and alveolar epithelia. *The Journal of Pathology*. 2021; 253: 17–30.
- [4] Vlahos R, Bozinovski S. Role of alveolar macrophages in chronic obstructive pulmonary disease. *Frontiers in Immunology*. 2014; 5: 435.
- [5] Lee J, Chun W, Lee HJ, Min J, Kim S, Seo J, *et al*. The Role of Macrophages in the Development of Acute and Chronic Inflammatory Lung Diseases. *Cells*. 2021; 10: 897.
- [6] Akata K, van Eeden SF. Lung Macrophage Functional Properties in Chronic Obstructive Pulmonary Disease. *International Journal of Molecular Sciences*. 2020; 21: 853.
- [7] Lea S, Gaskell R, Hall S, Maschera B, Hessel E, Singh D. Assessment of bacterial exposure on phagocytic capability and surface marker expression of sputum macrophages and neutrophils in COPD patients. *Clinical and Experimental Immunology*. 2021; 206: 99–109.
- [8] Li X, Zhao F, Wang A, Cheng P, Chen H. Role and mechanisms of autophagy in lung metabolism and repair. *Cellular and Molecular Life Sciences*. 2021; 78: 5051–5068.
- [9] Bagam P, Kaur G, Singh DP, Batra S. In vitro study of the role of FOXO transcription factors in regulating cigarette smoke extract-induced autophagy. *Cell Biology and Toxicology*. 2021; 37: 531–553.
- [10] Sarkar A, Tindle C, Pranadinata RF, Reed S, Eckmann L, Stappenbeck TS, *et al*. ELMO1 Regulates Autophagy Induction and Bacterial Clearance During Enteric Infection. *The Journal of Infectious Diseases*. 2017; 216: 1655–1666.
- [11] Vij N, Chandramani-Shivalingappa P, Van Westphal C, Hole R, Bodas M. Cigarette smoke-induced autophagy impairment accelerates lung aging, COPD-emphysema exacerbations and pathogenesis. *American Journal of Physiology. Cell Physiology*. 2018; 314: C73–C87.
- [12] Kono Y, Colley T, To M, Papaioannou AI, Mercado N, Baker JR, *et al*. Cigarette smoke-induced impairment of autophagy in macrophages increases galectin-8 and inflammation. *Scientific Reports*. 2021; 11: 335.
- [13] Tan Y, Zhang P, Feng Y, Yang Y, Liang W, Yang H, *et al*. Effects of GBE on the level of IL-1 and IL-8 in serum and bronchoalveolar lavage fluid of COPD rats. *China Journal of Modern Medicine*. 2018; 28: 7–10.
- [14] Li M, Chen Y, Cai W, Dong L, He F, Hong H, *et al*. Effects of Wenshen Yiqi Granules on the proliferation of airway smooth muscle cells and the expression of PI3K/AKT/mTOR signaling pathway in rats with CDPD. *China Journal of Traditional Chinese Medicine*. 2019; 4: 1711–1714.
- [15] Mavili HS, Isisag A, Tan A, Miskioglu M, Baraz LS, Nese N. Relationship of Tumor-Associated Macrophage Population Detected by CD68 PG-M1, CD68 KP1, and CD163 with Latent EBV Infection and Prognosis in Classical Hodgkin Lymphoma. *Turk Patoloji Dergisi*. 2021; 37: 130–138.
- [16] Klionsky DJ, Abdel-Aziz AK, Abdelfatah S, Abdellatif M, Abdoli A, Abel S, *et al*. Guidelines for the use and interpretation of assays for monitoring autophagy (4th edition)<sup>1</sup>. *Autophagy*. 2021; 17: 1–382.
- [17] Shubin AV, Demidyuk IV, Komissarov AA, Rafieva LM, Kostrov SV. Cytoplasmic vacuolization in cell death and survival. *Oncotarget*. 2016; 7: 55863–55889.
- [18] Henics T, Wheatley DN. Cytoplasmic vacuolation, adaptation and cell death: a view on new perspectives and features. *Biology of the Cell*. 1999; 91: 485–498.
- [19] Chen R, Duan C, Chen S, Zhang C, He T, Li H, *et al*. The suppressive role of p38 MAPK in cellular vacuole formation. *Journal of Cellular Biochemistry*. 2013; 114: 1789–1799.
- [20] Rodrigues SDO, Cunha CMCD, Soares GMV, Silva PL, Silva AR, Gonçalves-de-Albuquerque CF. Mechanisms, Pathophysiology and Currently Proposed Treatments of Chronic Obstructive Pulmonary Disease. *Pharmaceuticals*. 2021; 14: 979.
- [21] Wang L, Meng J, Wang C, Yang C, Wang Y, Li Y, *et al*. Hydrogen sulfide alleviates cigarette smoke-induced COPD through inhibition of the TGF- $\beta$ 1/smad pathway. *Experimental Biology and Medicine*. 2020; 245: 190–200.
- [22] Woo YD, Jeong D, Chung DH. Development and Functions of Alveolar Macrophages. *Molecules and Cells*. 2021; 44: 292–300.
- [23] Singh R, Belchamber KBR, Fenwick PS, Chana K, Donaldson G, Wedzicha JA, *et al*. Defective monocyte-derived macrophage phagocytosis is associated with exacerbation frequency in COPD. *Respiratory Research*. 2021; 22: 113.

- [24] Wang Y, Wang X, Wu P, Wang Y, Ren L, Xu A. Necroptosis Mediates Cigarette Smoke-Induced Inflammatory Responses in Macrophages. *International Journal of Chronic Obstructive Pulmonary Disease*. 2020; 15: 1093–1101.
- [25] Ghebre MA, Pang PH, Diver S, Desai D, Bafadhel M, Haldar K, *et al*. Biological exacerbation clusters demonstrate asthma and chronic obstructive pulmonary disease overlap with distinct mediator and microbiome profiles. *The Journal of Allergy and Clinical Immunology*. 2018; 141: 2027–2036.e12.
- [26] Yang D, Wang L, Jiang P, Kang R, Xie Y. Correlation between hs-CRP, IL-6, IL-10, ET-1, and Chronic Obstructive Pulmonary Disease Combined with Pulmonary Hypertension. *Journal of Healthcare Engineering*. 2022; 2022: 3247807.
- [27] Hikichi M, Mizumura K, Maruoka S, Gon Y. Pathogenesis of chronic obstructive pulmonary disease (COPD) induced by cigarette smoke. *Journal of Thoracic Disease*. 2019; 11: S2129–S2140.
- [28] Barnes PJ, Baker J, Donnelly LE. Autophagy in asthma and chronic obstructive pulmonary disease. *Clinical Science*. 2022; 136: 733–746.
- [29] Racanelli AC, Kikkers SA, Choi AMK, Cloonan SM. Autophagy and inflammation in chronic respiratory disease. *Autophagy*. 2018; 14: 221–232.
- [30] Tejwani V, Moughames E, Suresh K, Tang S, Mair LG, Romero K, *et al*. Black Carbon Content in Airway Macrophages is Associated with Reduced CD80 Expression and Increased Exacerbations in Former Smokers With COPD. *Chronic Obstructive Pulmonary Diseases*. 2021; 8: 91–99.
- [31] Huang H, Li N, Li D, Jing D, Liu Z, Xu X, *et al*. Autophagy Promotes Cigarette Smoke-Initiated and Elastin-Driven Bronchitis-Like Airway Inflammation in Mice. *Frontiers in Immunology*. 2021; 12: 594330.
- [32] Le Y, Wang Y, Zhou L, Xiong J, Tian J, Yang X, *et al*. Cigarette smoke-induced HMGB1 translocation and release contribute to migration and NF- $\kappa$ B activation through inducing autophagy in lung macrophages. *Journal of Cellular and Molecular Medicine*. 2020; 24: 1319–1331.
- [33] Sánchez-Martín P, Saito T, Komatsu M. p62/SQSTM1: ‘Jack of all trades’ in health and cancer. *The FEBS Journal*. 2019; 286: 8–23.
- [34] Elbially A. In vivo autophagy quantification: Measuring LC3 and P62 puncta in 3D image system from zebrafish larvae. *Journal of Cellular Biochemistry*. 2021; 122: 1435–1444.
- [35] Bo T, Kang Y, Liu Y, Xu J, Wang W. Atg5 Regulates Selective Autophagy of the Parental Macronucleus during *Tetrahymena* Sexual Reproduction. *Cells*. 2021; 10: 3071.
- [36] Hurley JH, Young LN. Mechanisms of Autophagy Initiation. *Annual Review of Biochemistry*. 2017; 86: 225–244.
- [37] Frangež Ž, Gérard D, He Z, Gavriil M, Fernández-Marrero Y, Seyed Jafari SM, *et al*. ATG5 and ATG7 Expression Levels Are Reduced in Cutaneous Melanoma and Regulated by NRF1. *Frontiers in Oncology*. 2021; 11: 721624.
- [38] Ma Y, Li C, He Y, Fu T, Song L, Ye Q, *et al*. Beclin-1/LC3-II dependent macroautophagy was uninfluenced in ischemia-challenged vascular endothelial cells. *Genes & Diseases*. 2021; 9: 549–561.
- [39] Huang Q, Liu Y, Zhang S, Yap YT, Li W, Zhang D, *et al*. Autophagy core protein ATG5 is required for elongating spermatid development, sperm individualization and normal fertility in male mice. *Autophagy*. 2021; 17: 1753–1767.
- [40] Satyavarapu EM, Nath S, Mandal C. Desialylation of Atg5 by sialidase (Neu2) enhances autophagosome formation to induce anchorage-dependent cell death in ovarian cancer cells. *Cell Death Discovery*. 2021; 7: 26.
- [41] Cai Q, Wang S, Jin L, Weng M, Zhou D, Wang J, *et al*. Long non-coding RNA GBCDR1nc1 induces chemoresistance of gallbladder cancer cells by activating autophagy. *Molecular Cancer*. 2019; 18: 82.
- [42] Collier JJ, Oláhová M, McWilliams TG, Taylor RW. ATG7 safeguards human neural integrity. *Autophagy*. 2021; 17: 2651–2653.
- [43] Fujita N, Huang W, Lin T, Groulx J, Jean S, Nguyen J, *et al*. Genetic screen in *Drosophila* muscle identifies autophagy-mediated T-tubule remodeling and a Rab2 role in autophagy. *eLife*. 2017; 6: e23367.
- [44] Lőrincz P, Tóth S, Benkő P, Lakatos Z, Boda A, Glatz G, *et al*. Rab2 promotes autophagic and endocytic lysosomal degradation. *The Journal of Cell Biology*. 2017; 216: 1937–1947.
- [45] Kuchitsu Y, Fukuda M. Revisiting Rab7 Functions in Mammalian Autophagy: Rab7 Knockout Studies. *Cells*. 2018; 7: 215.
- [46] Shi Z, Zhang M, Liu J, Zhang W, Hu D, Wang Q, *et al*. Autophagy Induced by BCL2-Related ceRNA Network Participates in the Occurrence of COPD. *International Journal of Chronic Obstructive Pulmonary Disease*. 2022; 17: 791–808.
- [47] Klionsky DJ, Abdelmohsen K, Abe A, Abedin MJ, Abeliovich H, Acevedo Arozena A, *et al*. Guidelines for the use and interpretation of assays for monitoring autophagy (3rd edition). *Autophagy*. 2016; 12: 1–222.
- [48] Liu Y, Xu J, Liu T, Wu J, Zhao J, Wang J, *et al*. FSTL1 aggravates cigarette smoke-induced airway inflammation and airway remodeling by regulating autophagy. *BMC Pulmonary Medicine*. 2021; 21: 45.
- [49] Monick MM, Powers LS, Walters K, Lovan N, Zhang M, Gerke A, *et al*. Identification of an autophagy defect in smokers’ alveolar macrophages. *Journal of Immunology*. 2010; 185: 5425–5435.
- [50] Zhang L, Huang J, Dong R, Feng Y, Zhou M. Therapeutic potential of BLT1 antagonist for COPD: involvement of inducing autophagy and ameliorating inflammation. *Drug Design, Development and Therapy*. 2019; 13: 3105–3116.